

# Anderson-Bogoliubov and Carlson-Goldman modes in counterflow superconductors. The case study of a double monolayer graphene.

K. V. Germash<sup>1</sup>, D. V. Fil<sup>1,2\*</sup>

<sup>1</sup>*Institute for Single Crystals, National Academy of Sciences of Ukraine, 60 Nauky Avenue, Kharkiv 61072, Ukraine*

<sup>2</sup>*V.N. Karazin Kharkiv National University, 4 Svobody Square, Kharkiv 61022, Ukraine*

The impact of electron-hole pairing on the spectrum of plasma excitations in double layer systems is investigated. The theory is developed with reference to a double monolayer graphene. Taking into account the coupling of scalar potential oscillations with oscillations of the order parameter  $\Delta$  we show that the spectrum of antisymmetric (acoustic) plasma excitations contains two modes, a weakly damped mode below the gap  $2\Delta$  and a strongly damped mode above the gap. The lower mode can be interpreted as an analog of the Carlson-Goldman mode. This mode has an acoustic dispersion relation at small wave vectors and it saturates at the level  $2\Delta$  at large wave vectors. Its velocity is larger than the velocity of the Anderson-Bogoliubov mode  $v_{AB} = v_F/\sqrt{2}$ , and it can be smaller than the Fermi velocity  $v_F$ . The damping rate of this mode strongly increases under increase of temperature. Out of phase oscillations of two order parameters in two spin subsystems are also considered. This part of the spectrum contains two more modes. One of them is interpreted as an analog of the Anderson-Bogoliubov (phase) mode and the other, as an analog of the Schmid (amplitude) mode. With minor modifications the theory can be extended to describes collective modes in a double bilayer graphene as well

## I. INTRODUCTION

Electron-hole pairing is a phenomenon analogous to the Cooper pairing that may occur in double layer systems consisting of an electron-doped and a hole-doped conducting layers<sup>1,2</sup> (see also Ref. 3 for a review). In the paired state the system may support dissipationless counterflow - a flow of oppositely directed superconducting electric currents in adjacent layers. The phenomenon is referred to as the superfluidity of spatially indirect excitons, exciton condensation in bilayers, or the counterflow superconductivity.

A strong increase of the counterflow conductivity at low temperature caused by the electron-hole pairing was observed<sup>4-6</sup> in quantum Hall bilayers with the total filling factor of one ( $\nu_T = 2\pi\ell_B^2(n_1 + n_2) = 1$ , where  $n_i$  is the electron density in the  $i$ -th layer and  $\ell_B$  is the magnetic length). The current state of art in experimental investigations of exciton condensation in  $\nu_T = 1$  quantum Hall bilayers is described in Ref. 7. Quantum Hall bilayers demonstrate a zero bias peak in the differential tunneling conductance<sup>8</sup> and a strong interlayer drag resistance<sup>9</sup>. These two features are considered as experimental signatures of the electron-hole pairing. Similar features were observed in double layer systems in zero magnetic field. The increase of the interlayer drag resistance at low temperature was detected in a double quantum well in AlGaAs heterostructures<sup>10,11</sup> and in hybrid double layer systems comprising a monolayer (bilayer) graphene in close proximity to a quantum well created in GaAs<sup>12</sup>. Experimental observation of strongly enhanced tunneling between two graphene bilayers at equal occupation of adjacent bilayers by electrons and holes was reported recently<sup>13</sup>. The registered tunneling conductance at small bias voltage was many orders of magnitude greater than that predicted for uncorrelated electrons and holes.

Theoretical consideration shows that promising candidates for a realization of electron-hole pairing in zero magnetic field are double monolayer<sup>14-19</sup>, double bilayer<sup>20-22</sup> and double multilayer<sup>23</sup> graphenes, double transition metal dichalcogenide monolayers<sup>24-26</sup>, phosphorene double layer<sup>27,28</sup> and topological insulators<sup>29,30</sup>.

In recent papers<sup>31-33</sup> we have predicted the effects that can be considered as additional hallmarks of the electron-hole pairing. It was shown<sup>31</sup> that the electron-hole pairing suppresses the ability of a double layer graphene system to screen the electrostatic field of an external charge. In the paired state at  $T = 0$  the electrostatic field remains completely unscreened at large distances. It was found<sup>32</sup> that the electron-hole pairing influences significantly the spectrum of plasma excitations in a double layer graphene system. Namely, instead of one optical (symmetric) plasmon mode two symmetric modes emerge. The frequency of the lower mode is restricted from above by the inequality  $\hbar\omega < 2\Delta$ , where  $2\Delta$  is the gap in the electron spectrum caused by the electron-hole pairing. This mode is a weakly damped one and its frequency is very sensitive to the temperature. At  $T = 0$  the lower mode disappears. On the contrary, the upper mode belongs to the frequency domain  $\hbar\omega > 2\Delta$ , it is strongly damped mode, its frequency is less sensitive to the temperature and it survives at  $T = 0$ . It was also established<sup>33</sup> that the electron-hole pairing provokes a huge increase of efficiency of the third-harmonic generation in double monolayer and double bilayer graphenes.

The results<sup>31-33</sup> were obtained within the approach that does not account the oscillations of the order parameter of the electron-hole pairing. It is known from the Bardeen-Cooper-Schrieffer theory of superconductivity<sup>34,35</sup> that neglecting the order parameter oscillations results in a violation of the gauge invariance of the polarization matrix. The gauge invariance is restored by “dressing” of the vertexes. The “dressed” vertexes should satisfy the generalized Ward identity. In Ref. 32 we have proposed a heuristic approach to the problem. We have obtained the gauge invariant polarization matrix using the vertex functions obtained as particular solutions of the generalized Ward identity.

In this paper we present the approach in which the order parameter oscillations are accounted explicitly. Our approach is close to one developed in Ref. 36 for conventional superconductors.

In Sec. II we introduce the model in which the electron-hole pairing is described by the order parameter independent of the momenta of paired quasiparticles. The perturbation Hamiltonian that accounts the order parameter oscillations is given in Sec. III. In Sec. IV the analytical expressions for the response functions and the polarization matrix are obtained. In Sec. V we derive the dispersion equation and calculate the eigenmode spectrum. We identify 6 modes. Two modes correspond to in-phase oscillations of the scalar potentials of two layers, that reproduces the result of Ref. 32. Two other modes correspond to out of phase oscillations of the scalar potentials coupled to in-phase oscillations of two order parameters (two order parameters describe pairing in two spin subsystems). One of these modes is interpreted as an analog of the Carlson-Goldman mode in superconductors. The rest two modes correspond to out of phase oscillations of two order parameters. They can be considered as analogs of the Anderson-Bogoliubov (phase) and Schmid (amplitude) modes in neutral superfluids and superconductors.

## II. THE MODEL

We consider the electron-hole pairing in a double monolayer graphene system where the concentration of electrons in one layer is equal to the concentration of holes in the other layer. We describe the pairing by the order parameter that is independent of the momentum. Such an order parameter can be defined self-consistently in the case of contact

interaction between electrons and holes<sup>16,17</sup>. In the model with contact interaction the eigenvalue problem for the collective mode spectrum can be reduced to a set of algebraic equations (for the momentum dependent order parameter the algebraic equations are transformed into integral ones).

We describe the system by the Hamiltonian

$$H = H_1 + H_2 + H_{12}, \quad (1)$$

where

$$H_n = -t \sum_{\sigma} \sum_{\langle ij \rangle} c_{n,i,\sigma}^+ c_{n,j,\sigma} - \mu_n \sum_{i,\sigma} c_{n,i,\sigma}^+ c_{n,i,\sigma} \quad (2)$$

is the single-layer Hamiltonian,  $c_{n,i,\sigma}^+$  and  $c_{n,i,\sigma}$  are the creation and annihilation operators of electrons,  $n = 1, 2$  is the layer index,  $i$  is the lattice site index,  $\sigma = \uparrow, \downarrow$  is the spin index,  $t$  is the nearest-neighbor hopping energy, and  $\mu_n$  is the electron chemical potential in the  $n$ -th layer. The chemical potentials are counted from the Dirac points and satisfy the condition  $\mu_1 = -\mu_2 = \mu$  that corresponds to equal concentrations of electrons and holes. The interaction part of the Hamiltonian reads

$$H_{12} = V \sum_{i,\sigma} c_{1,i,\sigma}^+ c_{2,i,\sigma}^+ c_{2,i,\sigma} c_{1,i,\sigma}, \quad (3)$$

where  $V$  is the interaction constant ( $V > 0$ ).

The order parameter of the electron-hole pairing is defined as

$$\Delta_{i,\sigma} = V \langle c_{2,i,\sigma}^+ c_{1,i,\sigma} \rangle. \quad (4)$$

The order parameter can be presented as a sum of the equilibrium part  $\Delta_{i,\sigma}^{(0)}$  and the fluctuating part  $\Delta_{i,\sigma}^{(fl)}(t)$ . We consider the paired state with the lowest energy<sup>16,17</sup> that corresponds to the choice  $\Delta_{i_A,\sigma}^{(0)} = -\Delta_{i_B,\sigma}^{(0)} = \Delta$ , where  $i_A$  and  $i_B$  stand for the sites in the  $i$ -th unit cell belonging to two different graphene sublattices.

Neglecting the order parameter oscillations we obtain the mean-field Hamiltonian

$$H_{MF} = H_1 + H_2 - \sum_{i,\sigma} (\Delta c_{1,i_A,\sigma}^+ c_{2,i_A,\sigma} - \Delta c_{1,i_B,\sigma}^+ c_{2,i_B,\sigma} + H.c.). \quad (5)$$

Here and below  $i$  stands for the unit cell index. Applying the Fourier-transformation to the Hamiltonian (5) and considering one spin component we get

$$H_{MF} = \sum_{\mathbf{k}} \Psi_{\mathbf{k}}^+ h_{\mathbf{k}} \Psi_{\mathbf{k}} = \sum_{\mathbf{k}} \begin{pmatrix} c_{1,A,\mathbf{k}}^+ & c_{1,B,\mathbf{k}}^+ & c_{2,A,\mathbf{k}}^+ & c_{2,B,\mathbf{k}}^+ \end{pmatrix} \begin{pmatrix} -\mu & f_{\mathbf{k}} & -\Delta & 0 \\ f_{\mathbf{k}}^* & -\mu & 0 & \Delta \\ -\Delta & 0 & \mu & f_{\mathbf{k}} \\ 0 & \Delta & f_{\mathbf{k}}^* & \mu \end{pmatrix} \begin{pmatrix} c_{1,A,\mathbf{k}} \\ c_{1,B,\mathbf{k}} \\ c_{2,A,\mathbf{k}} \\ c_{2,B,\mathbf{k}} \end{pmatrix}, \quad (6)$$

where  $c_{n,A(B),\mathbf{k}} = (1/\sqrt{N}) \sum_i c_{n,i_{A(B)}} e^{i\mathbf{k}\mathbf{R}_i}$  is the Fourier-transformed annihilation operator (here we omit the spin index), the creation operator is given by the Hermitian conjugate,  $N$  is the total number of unit cells, and  $f_{\mathbf{k}} = |f_{\mathbf{k}}| e^{i\chi_{\mathbf{k}}} = -t \sum_{j=1,2,3} e^{-i\mathbf{k}\vec{\delta}_j}$  with  $\vec{\delta}_1 = \mathbf{a}_1$ ,  $\vec{\delta}_2 = \mathbf{a}_2$ ,  $\vec{\delta}_3 = 0$  ( $\mathbf{a}_1$  and  $\mathbf{a}_2$  are the primitive lattice vectors).

The Hamiltonian (6) is diagonalized by the unitary transformation

$$H_{MF} = \sum_{\mathbf{k}} \Psi_{\mathbf{k}}^+ \hat{U}_{\mathbf{k}}^{-1} \hat{U}_{\mathbf{k}} h_{\mathbf{k}} \hat{U}_{\mathbf{k}}^{-1} \hat{U}_{\mathbf{k}} \Psi_{\mathbf{k}} = \sum_{\mathbf{k}} \tilde{\Psi}_{\mathbf{k}}^+ \tilde{h}_{\mathbf{k}} \tilde{\Psi}_{\mathbf{k}}, \quad (7)$$

where  $\tilde{h}_{\mathbf{k}} = \hat{U}_{\mathbf{k}} h_{\mathbf{k}} \hat{U}_{\mathbf{k}}^{-1}$  and  $\tilde{\Psi}_{\mathbf{k}} = \hat{U}_{\mathbf{k}} \Psi_{\mathbf{k}}$ . The matrix  $\hat{U}_{\mathbf{k}}$  can be written in a form of the product

$$\hat{U}_{\mathbf{k}} = \hat{U}_{uv} \hat{U}_b \hat{U}_{\chi}. \quad (8)$$

The matrix

$$\hat{U}_{\chi} = \frac{1}{\sqrt{2}} \begin{pmatrix} 1 & e^{i\chi_{\mathbf{k}}} & 0 & 0 \\ 1 & -e^{i\chi_{\mathbf{k}}} & 0 & 0 \\ 0 & 0 & 1 & e^{i\chi_{\mathbf{k}}} \\ 0 & 0 & 1 & -e^{i\chi_{\mathbf{k}}} \end{pmatrix} \quad (9)$$

diagonalizes the single-layer parts of the Hamiltonian. The matrix

$$\hat{U}_b = \begin{pmatrix} 1 & 0 & 0 & 0 \\ 0 & 0 & 0 & 1 \\ 0 & 1 & 0 & 0 \\ 0 & 0 & 1 & 0 \end{pmatrix} \quad (10)$$

rearranges the elements of the matrix  $\hat{U}_\chi h_{\mathbf{k}} \hat{U}_\chi^{-1}$  into two blocks:

$$\hat{U}_b \hat{U}_\chi h_{\mathbf{k}} \hat{U}_\chi^{-1} \hat{U}_b^{-1} = \begin{pmatrix} \xi_{\mathbf{k},+1} & -\Delta & 0 & 0 \\ -\Delta & -\xi_{\mathbf{k},+1} & 0 & 0 \\ 0 & 0 & \xi_{\mathbf{k},-1} & -\Delta \\ 0 & 0 & -\Delta & -\xi_{\mathbf{k},-1} \end{pmatrix}, \quad (11)$$

where  $\xi_{\mathbf{k},\lambda} = \lambda|f_{\mathbf{k}}| - \mu$ , and  $\lambda = \pm 1$ .

Each block can be diagonalized by the u-v transformation. The matrix

$$\hat{U}_{uv} = \begin{pmatrix} u_{\mathbf{k},+1} & -v_{\mathbf{k},+1} & 0 & 0 \\ v_{\mathbf{k},+1} & u_{\mathbf{k},+1} & 0 & 0 \\ 0 & 0 & u_{\mathbf{k},-1} & -v_{\mathbf{k},-1} \\ 0 & 0 & v_{\mathbf{k},-1} & u_{\mathbf{k},-1} \end{pmatrix} \quad (12)$$

is expressed through the coefficients of this transformation:

$$u_{\mathbf{k},\lambda} = \sqrt{\frac{1}{2} \left( 1 + \frac{\xi_{\mathbf{k},\lambda}}{E_{\mathbf{k},\lambda}} \right)}, \quad v_{\mathbf{k},\lambda} = \sqrt{\frac{1}{2} \left( 1 - \frac{\xi_{\mathbf{k},\lambda}}{E_{\mathbf{k},\lambda}} \right)}, \quad (13)$$

where  $E_{\mathbf{k},\lambda} = \sqrt{\xi_{\mathbf{k},\lambda}^2 + \Delta^2}$ .

The transformed Hamiltonian has the diagonal form:

$$H_{MF} = \sum_{\nu} E_{\nu} \alpha_{\nu}^{\dagger} \alpha_{\nu}, \quad (14)$$

where  $\nu = (\mathbf{k}, \lambda, m)$  (with  $m = \pm 1$ ) is the full set of the quasiparticle quantum numbers, excluding spin,  $E_{\nu} = mE_{\mathbf{k},\lambda}$  is the quasiparticle energy, and  $\alpha_{\nu}^{\dagger}$ ,  $\alpha_{\nu}$  are the quasiparticle creation and annihilation operators.

Applying to Eq. (4) the Fourier-transformation and the unitary transformation  $\hat{U}_{\mathbf{k}}$  we obtain the following equation for the order parameter

$$\Delta = -\frac{V}{2N} \sum_{\nu} m u_{\mathbf{k},\lambda} v_{\mathbf{k},\lambda} \langle \alpha_{\nu}^{\dagger} \alpha_{\nu} \rangle. \quad (15)$$

Replacing the average  $\langle \alpha_{\nu}^{\dagger} \alpha_{\nu} \rangle$  with the Fermi distribution function we arrive at the self-consistence equation

$$\Delta = \frac{V\Omega_0}{2S} \sum_{\mathbf{k},\lambda} \frac{\Delta}{2E_{\mathbf{k},\lambda}} \tanh \frac{E_{\mathbf{k},\lambda}}{2T}, \quad (16)$$

where  $\Omega_0$  is the area of the unit cell and  $S$  is the area of the system.

We emphasize that Eq. (16) differs from one obtained in the model with a long-range Coulomb interaction<sup>14,15,18,19</sup>. In the latter case the self-consistence equation has the form

$$\Delta_{\mathbf{k},\lambda} = \frac{1}{S} \sum_{\mathbf{k}',\lambda'} V(\mathbf{k} - \mathbf{k}') \frac{1 + \lambda\lambda' \cos(\chi_{\mathbf{k}} - \chi_{\mathbf{k}'})}{2} \frac{\Delta_{\mathbf{k}',\lambda'}}{2E_{\mathbf{k}',\lambda'}} \tanh \frac{E_{\mathbf{k}',\lambda'}}{2T}, \quad (17)$$

where  $V(\mathbf{q})$  is the Fourier-component of the interlayer Coulomb interaction. In difference with Eq. (16), the order parameter independent of  $\mathbf{k}$  and  $\lambda$  does not satisfy Eq. (17).

### III. PERTURBATION HAMILTONIAN

Now we add to the Hamiltonian (6) the perturbation part  $H_{int}$ . The perturbation Hamiltonian  $H_{int}$  describes the oscillations of the order parameter and the interaction of electrons with the scalar potential  $\varphi(\mathbf{r}, t)$ . We consider the oscillations for which  $\Delta_{iA,\sigma}^{(fl)}(t) = -\Delta_{iB,\sigma}^{(fl)}(t) = \Delta_{i,\sigma}^{(fl)}(t)$  ( $i$  is the unit cell index) and do not account oscillations with  $\Delta_{iA,\sigma}^{(fl)} = \Delta_{iB,\sigma}^{(fl)}$ . The latter ones are decoupled from the scalar potential oscillations and do not modify the response to the electromagnetic field.

The Fourier-components of the real and imaginary parts of the order parameter oscillations are defined as

$$\Delta_1(\mathbf{q}, \omega) = \Omega_0 \sum_i \int dt e^{i\omega t - i\mathbf{q}\mathbf{R}_i} \text{Re}[\Delta_i^{(fl)}(t)], \quad (18)$$

$$\Delta_2(\mathbf{q}, \omega) = \Omega_0 \sum_i \int dt e^{i\omega t - i\mathbf{q}\mathbf{R}_i} \text{Im}[\Delta_i^{(fl)}(t)]. \quad (19)$$

We specify the case of real-valued  $\Delta$  (it is accounted in the Hamiltonian (6) and in the coefficient (13)). Then the quantities  $\Delta_1$  and  $\Delta_2$  describe small oscillations of the amplitude and the phase of the order parameter, respectively.

The perturbation Hamiltonian can be presented in the matrix form

$$H_{int}(t) = -\frac{1}{2\pi S} \sum_{\mathbf{k}, \mathbf{q}} \int d\omega e^{-i\omega t} \Psi_{\mathbf{k}-\mathbf{q}}^+ \left[ \frac{e}{2} \varphi_+(\mathbf{q}, \omega) \hat{T}^{(0)} + \Delta_1(\mathbf{q}, \omega) \hat{T}^{(1)} + \Delta_2(\mathbf{q}, \omega) \hat{T}^{(2)} + \frac{e}{2} \varphi_-(\mathbf{q}, \omega) \hat{T}^{(3)} \right] \Psi_{\mathbf{k}}, \quad (20)$$

where the operators  $\Psi_{\mathbf{k}}^+$  and  $\Psi_{\mathbf{k}}$  are defined by Eq. (6),

$$\varphi_{\pm}(\mathbf{q}, \omega) = \Omega_0 \sum_i \int dt e^{i\omega t - i\mathbf{q}\mathbf{R}_i} [\varphi_1(\mathbf{R}_i, t) \pm \varphi_2(\mathbf{R}_i, t)] \quad (21)$$

is the Fourier-component of the sum (difference) of the scalar potentials in two graphene layers, and  $\varphi_n(\mathbf{R}_i, t)$  is the scalar potentials in the  $n$ -th layer in the  $i$ -th unit cell. The matrixes  $\hat{T}^{(s)}$  in Eq. (20) are expressed through the Pauli matrix  $\hat{\sigma}_z$  and the identity matrix  $\hat{I}$ :

$$\hat{T}^{(0)} = \begin{pmatrix} \hat{I} & 0 \\ 0 & \hat{I} \end{pmatrix}, \quad \hat{T}^{(1)} = \begin{pmatrix} 0 & \hat{\sigma}_z \\ \hat{\sigma}_z & 0 \end{pmatrix}, \quad \hat{T}^{(2)} = \begin{pmatrix} 0 & i\hat{\sigma}_z \\ -i\hat{\sigma}_z & 0 \end{pmatrix}, \quad \hat{T}^{(3)} = \begin{pmatrix} \hat{I} & 0 \\ 0 & -\hat{I} \end{pmatrix}. \quad (22)$$

We apply the transformation (7) to the Hamiltonian (20) and write it through the operators of creation and annihilation of quasiparticle excitations:

$$H_{int}(t) = \frac{1}{2\pi S} \sum_{\nu_1, \nu_2} \int d\omega e^{-i\omega t} \alpha_{\nu_1}^+ [h_{int}(\omega)]_{\nu_1, \nu_2} \alpha_{\nu_2}, \quad (23)$$

where

$$[h_{int}(\omega)]_{\nu_1, \nu_2} = -\frac{e}{2} \varphi_+(\mathbf{k}_2 - \mathbf{k}_1, \omega) R_{\nu_1, \nu_2}^{(0)} - \Delta_1(\mathbf{k}_2 - \mathbf{k}_1, \omega) R_{\nu_1, \nu_2}^{(1)} - \Delta_2(\mathbf{k}_2 - \mathbf{k}_1, \omega) R_{\nu_1, \nu_2}^{(2)} - \frac{e}{2} \varphi_-(\mathbf{k}_2 - \mathbf{k}_1, \omega) R_{\nu_1, \nu_2}^{(3)}, \quad (24)$$

the matrixes  $R_{\nu_1, \nu_2}^{(s)}$  ( $s = 0, 1, 2, 3$ ) are given by the equation

$$R_{\mathbf{k}_1, \lambda_1, m_1; \mathbf{k}_2, \lambda_2, m_2}^{(s)} = \frac{1 + \lambda_1 \lambda_2 e^{i(\chi_{\mathbf{k}_1} - \chi_{\mathbf{k}_2})}}{2} [M^{(s)}(\mathbf{k}_1, \lambda_1, \mathbf{k}_2, \lambda_2)]_{i_{m_1}, i_{m_2}}, \quad (25)$$

( $i_{+1} \equiv 1, i_{-1} \equiv 2$ ) and the matrixes  $\hat{M}^{(s)}$  are expressed through the product

$$\hat{M}^{(s)}(\mathbf{k}_1, \lambda_1, \mathbf{k}_2, \lambda_2) = \begin{pmatrix} u_{\mathbf{k}_1, \lambda_1} & -v_{\mathbf{k}_1, \lambda_1} \\ v_{\mathbf{k}_1, \lambda_1} & u_{\mathbf{k}_1, \lambda_1} \end{pmatrix} \hat{\sigma}^{(s)} \begin{pmatrix} u_{\mathbf{k}_2, \lambda_2} & v_{\mathbf{k}_2, \lambda_2} \\ -v_{\mathbf{k}_2, \lambda_2} & u_{\mathbf{k}_2, \lambda_2} \end{pmatrix} \quad (26)$$

with  $\hat{\sigma}^{(0)} = \hat{I}$ ,  $\hat{\sigma}^{(1)} = \hat{\sigma}_x$ ,  $\hat{\sigma}^{(2)} = -\hat{\sigma}_y$ ,  $\hat{\sigma}^{(3)} = \hat{\sigma}_z$ .

#### IV. POLARIZATION MATRIX

Taking into account two spin components we write the Hamiltonian in the form

$$H(t) = H_{MF} + H_{int}(t) = \sum_{\nu,\sigma} E_{\nu} \alpha_{\nu,\sigma}^+ \alpha_{\nu,\sigma} + \frac{1}{2\pi S} \sum_{\nu_1,\nu_2,\sigma} \int d\omega e^{-i\omega t} \alpha_{\nu_1,\sigma}^+ [h_{int,\sigma}(\omega)]_{\nu_1,\nu_2} \alpha_{\nu_2,\sigma}, \quad (27)$$

where  $[h_{int,\sigma}(\omega)]_{\nu_1,\nu_2}$  is given by Eq. (24) with  $\Delta_{1(2)}(\mathbf{k}, \omega) \equiv \Delta_{1(2),\sigma}(\mathbf{k}, \omega)$ .

To calculate the response of the system to the scalar potential and to the order parameter oscillations we define the response functions

$$\eta_{\sigma}^{(s)}(\mathbf{q}, \omega) = \int dt e^{i\omega t} \sum_{\mathbf{k}} \langle \Psi_{\mathbf{k}+\mathbf{q},\sigma}^+ \hat{T}^{(s)} \Psi_{\mathbf{k},\sigma} \rangle, \quad (28)$$

where  $\Psi_{\mathbf{k},\sigma}^+$  and  $\Psi_{\mathbf{k},\sigma}$  are the same operators as in Eq. (6) with restored spin indexes. The angle brackets mean the quantum mechanical and thermodynamic average. We compute the averages in Eq. (28) using the density matrix formalism. The density matrix  $\hat{\rho}(t)$  satisfies the equation

$$\frac{\partial \hat{\rho}(t)}{\partial t} = \frac{1}{i\hbar} [H(t), \hat{\rho}(t)] - \gamma(\hat{\rho}(t) - \hat{\rho}_0), \quad (29)$$

where  $\hat{\rho}_0$  is the density matrix of the system described by the Hamiltonian  $H_{MF}$ , and  $\gamma$  is the relaxation rate. The averages in Eq. (28) are calculated as

$$\langle \Psi_{\mathbf{k}+\mathbf{q},\sigma}^+ \hat{T}^{(s)} \Psi_{\mathbf{k},\sigma} \rangle = \text{Tr} \left( [\hat{\rho}(t)]_{\mathbf{k},\sigma;\mathbf{k}+\mathbf{q},\sigma} \hat{T}^{(s)} \right), \quad (30)$$

where the trace is taken over the sublattice and layer indexes.

In the quasiparticle basis the response functions (28) are expressed as

$$\eta_{\sigma}^{(s)}(\mathbf{q}, \omega) = \sum_{\nu_1,\nu_2} [\hat{\rho}(\omega)]_{\nu_1,\sigma;\nu_2,\sigma} R_{\nu_2,\nu_1}^{(s)} \delta_{\mathbf{k}_2,\mathbf{k}_1+\mathbf{q}}, \quad (31)$$

where  $\hat{\rho}(\omega) = \int dt \exp(i\omega t) \hat{\rho}(t)$  and the matrixes  $R_{\nu_1,\nu_2}^{(s)}$  are given by Eq. (25).

The density matrix is sought in a form of expansion in powers of the perturbation Hamiltonian:  $\hat{\rho}(\omega) = \hat{\rho}_0(\omega) + \hat{\rho}_1(\omega) + \dots$ . The zero order term in this expansion is the equilibrium density matrix

$$[\hat{\rho}_0(\omega)]_{\nu_1,\sigma_1;\nu_2,\sigma_2} = 2\pi \delta(\omega) \delta_{\nu_1,\nu_2} \delta_{\sigma_1,\sigma_2} f_{\nu_1}, \quad (32)$$

where  $f_{\nu} = (e^{E_{\nu}/T} + 1)^{-1}$  is the Fermi distribution function. The first order term reads

$$[\hat{\rho}_1(\omega)]_{\nu_1,\sigma_1;\nu_2,\sigma_2} = \frac{1}{S} \frac{f_{\nu_1} - f_{\nu_2}}{E_{\nu_1} - E_{\nu_2} - \hbar(\omega + i\gamma)} [h_{int,\sigma_1}(\omega)]_{\nu_1,\nu_2} \delta_{\sigma_1,\sigma_2}. \quad (33)$$

The response functions  $\eta^{(0)}$  and  $\eta^{(3)}$  at  $\mathbf{q} \neq 0$  correspond to the charge density oscillations  $\rho_{\pm,\sigma} = \rho_{1,\sigma} \pm \rho_{2,\sigma}$ :

$$\rho_{+,\sigma}(\mathbf{q}, \omega) = -e\eta_{\sigma}^{(0)}(\mathbf{q}, \omega), \quad \rho_{-,\sigma}(\mathbf{q}, \omega) = -e\eta_{\sigma}^{(3)}(\mathbf{q}, \omega). \quad (34)$$

Taking into account the definition of the order parameter Eq. (4) we obtain the relation between the order parameter oscillations and the response functions  $\eta^{(1(2))}$  at  $\mathbf{q} \neq 0$ :

$$\Delta_{1,\sigma}(\mathbf{q}, \omega) = g\eta_{\sigma}^{(1)}(\mathbf{q}, \omega), \quad \Delta_{2,\sigma}(\mathbf{q}, \omega) = g\eta_{\sigma}^{(2)}(\mathbf{q}, \omega), \quad (35)$$

where  $g = V\Omega_0/4$  is the coupling constant.

Restricting with the linear response approximation we obtain from Eqs. (31), (33), (34), (35) the following matrix equation

$$\begin{pmatrix} e^{-1}\rho_{+,\sigma}(\mathbf{q}, \omega) \\ -g^{-1}\Delta_{1,\sigma}(\mathbf{q}, \omega) \\ -g^{-1}\Delta_{2,\sigma}(\mathbf{q}, \omega) \\ e^{-1}\rho_{-,\sigma}(\mathbf{q}, \omega) \end{pmatrix} = \begin{pmatrix} \Pi_{00}(\mathbf{q}, \omega) & \Pi_{01}(\mathbf{q}, \omega) & \Pi_{02}(\mathbf{q}, \omega) & \Pi_{03}(\mathbf{q}, \omega) \\ \Pi_{10}(\mathbf{q}, \omega) & \Pi_{11}(\mathbf{q}, \omega) & \Pi_{12}(\mathbf{q}, \omega) & \Pi_{13}(\mathbf{q}, \omega) \\ \Pi_{20}(\mathbf{q}, \omega) & \Pi_{21}(\mathbf{q}, \omega) & \Pi_{22}(\mathbf{q}, \omega) & \Pi_{23}(\mathbf{q}, \omega) \\ \Pi_{30}(\mathbf{q}, \omega) & \Pi_{31}(\mathbf{q}, \omega) & \Pi_{32}(\mathbf{q}, \omega) & \Pi_{33}(\mathbf{q}, \omega) \end{pmatrix} \begin{pmatrix} e\varphi_{+}(\mathbf{q}, \omega)/2 \\ \Delta_{1,\sigma}(\mathbf{q}, \omega) \\ \Delta_{2,\sigma}(\mathbf{q}, \omega) \\ e\varphi_{-}(\mathbf{q}, \omega)/2 \end{pmatrix}, \quad (36)$$

where the components of the polarization matrix are given by the expression

$$\Pi_{s_1 s_2}(\mathbf{q}, \omega) = \frac{1}{S} \sum_{\nu_1, \nu_2} \delta_{\mathbf{k}_2, \mathbf{k}_1 + \mathbf{q}} \Phi_{\nu_1 \nu_2}^{s_1 s_2} \frac{1 + \lambda_1 \lambda_2 \cos(\chi_{\mathbf{k}_1} - \chi_{\mathbf{k}_2})}{2} \frac{f_{\nu_1} - f_{\nu_2}}{E_{\nu_1} - E_{\nu_2} - \hbar(\omega + i\gamma)}. \quad (37)$$

The factors  $\Phi_{\nu_1 \nu_2}^{s_1 s_2}$  in Eq. (37) are expressed through the matrix (26):

$$\Phi_{\nu_1 \nu_2}^{s_1 s_2} = [\hat{M}^{(s_2)}(\mathbf{k}_1, \lambda_1, \mathbf{k}_2, \lambda_2)]_{i_{m_1}, i_{m_2}} [\hat{M}^{(s_1)}(\mathbf{k}_2, \lambda_2, \mathbf{k}_1, \lambda_1)]_{i_{m_2}, i_{m_1}}, \quad (38)$$

(there is no summation over repeated indexes in Eq. (38)).

From Eq. (38) we obtain the following explicit expressions for  $\Phi_{\nu_1 \nu_2}^{s_1 s_2}$  :

$$\begin{aligned} \Phi_{\nu_1 \nu_2}^{00} &= \frac{1}{2} \left( 1 + \frac{\xi_1 \xi_2 + \Delta^2}{E_1 E_2} \right), & \Phi_{\nu_1 \nu_2}^{01} &= -\frac{\Delta}{2} \left( \frac{1}{E_1} + \frac{1}{E_2} \right), & \Phi_{\nu_1 \nu_2}^{02} &= i \frac{\Delta}{2} \frac{\xi_2 - \xi_1}{E_2 E_1}, & \Phi_{\nu_1 \nu_2}^{03} &= \frac{1}{2} \left( \frac{\xi_2}{E_2} + \frac{\xi_1}{E_1} \right), \\ \Phi_{\nu_1 \nu_2}^{11} &= \frac{1}{2} \left( 1 - \frac{\xi_1 \xi_2 - \Delta^2}{E_1 E_2} \right), & \Phi_{\nu_1 \nu_2}^{12} &= \frac{i}{2} \left( \frac{\xi_1}{E_1} - \frac{\xi_2}{E_2} \right), & \Phi_{\nu_1 \nu_2}^{13} &= -\frac{\Delta}{2} \frac{\xi_1 + \xi_2}{E_1 E_2}, \\ \Phi_{\nu_1 \nu_2}^{22} &= \frac{1}{2} \left( 1 - \frac{\xi_1 \xi_2 + \Delta^2}{E_1 E_2} \right), & \Phi_{\nu_1 \nu_2}^{23} &= i \frac{\Delta}{2} \left( \frac{1}{E_2} - \frac{1}{E_1} \right), \\ \Phi_{\nu_1 \nu_2}^{33} &= \frac{1}{2} \left( 1 + \frac{\xi_1 \xi_2 - \Delta^2}{E_1 E_2} \right) \end{aligned} \quad (39)$$

and  $\Phi_{\nu_1 \nu_2}^{s_2, s_1} = (\Phi_{\nu_1 \nu_2}^{s_1, s_2})^*$ . Here we use the notations  $\xi_i \equiv \xi_{\nu_i}$  and  $E_i \equiv E_{\nu_i}$ .

Taking into account symmetry properties of the expression under summation in Eq. (37) one can show that some elements of the polarization matrix, namely,  $\Pi_{01}(\mathbf{q}, \omega)$ ,  $\Pi_{02}(\mathbf{q}, \omega)$ ,  $\Pi_{03}(\mathbf{q}, \omega)$ ,  $\Pi_{10}(\mathbf{q}, \omega)$ ,  $\Pi_{20}(\mathbf{q}, \omega)$ , and  $\Pi_{30}(\mathbf{q}, \omega)$  are equal to zero exactly.

## V. COLLECTIVE MODES

In the nonretarded approximation the scalar potential satisfies the Poisson equation

$$\nabla[\varepsilon(\mathbf{r})\nabla\varphi(\mathbf{r}, t)] = -4\pi\rho(\mathbf{r}, t), \quad (40)$$

where  $\varepsilon(\mathbf{r})$  is the space-dependent dielectric constant. We imply that the system consists of two graphene layers separated by a dielectric layer with the dielectric constant  $\varepsilon$  and surrounded by a medium with  $\varepsilon = 1$ . Then

$$\varepsilon(\mathbf{r}) = \begin{cases} 1, & z < -d/2; \\ \varepsilon, & -d/2 < z < d/2; \\ 1, & z > d/2, \end{cases} \quad (41)$$

where  $d$  is the distance between graphene layers, and the  $z$ -axis is directed perpendicular to graphene layers.

To obtain the eigenmode spectrum we account in Eq. (40) the charges induced in graphene layers by the scalar potential and by the order parameter oscillations:

$$\rho(\mathbf{r}, t) = \sum_{\sigma} [\rho_{1,\sigma}(\mathbf{r}_{pl}, t)\delta(z - d/2) + \rho_{2,\sigma}(\mathbf{r}_{pl}, t)\delta(z + d/2)], \quad (42)$$

where  $\mathbf{r}_{pl}$  is two-dimensional radius-vector in the  $(x, y)$ -plane.

Making the Fourier-transformation of Eq. (40) we obtain the equation for  $\varphi(\mathbf{q}, z, \omega)$ . Its solution yields the relation between the potentials  $\varphi_{\pm}(\mathbf{q}, \omega) = \varphi(\mathbf{q}, d/2, \omega) \pm \varphi(\mathbf{q}, -d/2, \omega)$  and the charge densities  $\rho_{\pm}(\mathbf{q}, \omega) = \sum_{\sigma} \rho_{\pm, \sigma}(\mathbf{q}, \omega)$ :

$$e^2 \varphi_{\pm}(\mathbf{q}, \omega) = V_{\pm}(q) \rho_{\pm}(\mathbf{q}, \omega), \quad (43)$$

where

$$V_{\pm}(q) = \frac{4\pi e^2}{q} \frac{1 \pm e^{-qd}}{(\varepsilon + 1) \mp (\varepsilon - 1)e^{-qd}} \quad (44)$$

are the Fourier-components of the Coulomb interaction energies  $V_{\pm}(r_{pl}) = V_{11}(r_{pl}) \pm V_{12}(r_{pl})$ . Here  $V_{11}(r_{pl})$  and  $V_{12}(r_{pl})$  are the energies of interaction of two electrons located in the same and different layers, correspondingly (we account that in the uniform dielectric environment  $V_{11}(r_{pl}) = V_{22}(r_{pl})$ ).

From Eqs. (36) and (43) we get the equation for the scalar potential and order parameter oscillations:

$$\begin{pmatrix} 2\Pi_{00} - \frac{2}{V_+(q)} & 0 & 0 & 0 & 0 & 0 \\ 0 & \Pi_{11} + \frac{1}{g} & \Pi_{12} & 0 & 0 & \Pi_{13} \\ 0 & \Pi_{21} & \Pi_{22} + \frac{1}{g} & 0 & 0 & \Pi_{23} \\ 0 & 0 & 0 & \Pi_{11} + \frac{1}{g} & \Pi_{12} & \Pi_{13} \\ 0 & 0 & 0 & \Pi_{21} & \Pi_{22} + \frac{1}{g} & \Pi_{23} \\ 0 & \Pi_{31} & \Pi_{32} & \Pi_{31} & \Pi_{32} & 2\Pi_{33} - \frac{2}{V_-(q)} \end{pmatrix} \begin{pmatrix} e\varphi_+(\mathbf{q}, \omega)/2 \\ \Delta_{1,\uparrow}(\mathbf{q}, \omega) \\ \Delta_{2,\uparrow}(\mathbf{q}, \omega) \\ \Delta_{1,\downarrow}(\mathbf{q}, \omega) \\ \Delta_{2,\downarrow}(\mathbf{q}, \omega) \\ e\varphi_-(\mathbf{q}, \omega)/2 \end{pmatrix} = 0, \quad (45)$$

where  $\Pi_{\alpha\beta} \equiv \Pi_{\alpha\beta}(\mathbf{q}, \omega)$ .

We calculate the polarization functions Eq. (37) in the Dirac approximation for the electron spectrum. In this approximation the sum over  $\mathbf{k}$  is replaced with the integral over two separate circles in the Brillouin zone centered at the Dirac points  $K$  and  $K'$ . In these circles  $|f(\mathbf{k})| \approx \hbar v_F k'$ , and  $\chi_{\mathbf{k}} \approx \mp \theta_{\mathbf{k}'}$ , where  $\mathbf{k}'$  is counted from the corresponding Dirac point,  $\theta_{\mathbf{k}'}$  is the angle between  $\mathbf{k}'$  and the  $x$ -axis, and  $v_F$  is the Fermi velocity in graphene. In the Dirac approximation the integrals in the expressions for  $\Pi_{11}(\mathbf{q}, \omega)$  and  $\Pi_{22}(\mathbf{q}, \omega)$  diverge at  $k' \rightarrow \infty$ . To overcome this problem we account the equality

$$\frac{1}{g} = \frac{1}{S} \sum_{\mathbf{k}, \lambda} \frac{1}{E_{\mathbf{k}, \lambda}} \tanh \frac{E_{\mathbf{k}, \lambda}}{2T} = -\frac{1}{S} \sum_{m, \mathbf{k}, \lambda} \frac{f_{m, \mathbf{k}, \lambda} - f_{-m, \mathbf{k}, \lambda}}{E_{m, \mathbf{k}, \lambda} - E_{-m, \mathbf{k}, \lambda}} \quad (46)$$

that follows from the self-consistence equation (16). Using the relation (46) we present the quantities  $\Pi_{ss}(\mathbf{q}, \omega) + 1/g$  ( $s = 1, 2$ ) in the form

$$\Pi_{ss}(\mathbf{q}, \omega) + \frac{1}{g} = \Pi_{ss}^{(R)}(\mathbf{q}, \omega) = \frac{1}{S} \sum_{\nu_1, \nu_2} \left[ \delta_{\mathbf{k}_2, \mathbf{k}_1 + \mathbf{q}} \Phi_{\nu_1 \nu_2}^{ss} \frac{1 + \lambda_1 \lambda_2 \cos(\chi_{\mathbf{k}_1} - \chi_{\mathbf{k}_2})}{2} \frac{f_{\nu_1} - f_{\nu_2}}{E_{\nu_1} - E_{\nu_2} - \hbar(\omega + i\gamma)} - \delta_{\mathbf{k}_1, \mathbf{k}_2} \delta_{m_1, -m_2} \delta_{\lambda_1, \lambda_2} \frac{f_{\nu_1} - f_{\nu_2}}{E_{\nu_1} - E_{\nu_2}} \right]. \quad (47)$$

The functions  $\Pi_{11}^{(R)}(\mathbf{q}, \omega)$  and  $\Pi_{22}^{(R)}(\mathbf{q}, \omega)$  calculated in the Dirac approximation do not diverge in the limit  $k' \rightarrow \infty$ . Equating the determinant of the matrix in Eq. (45) to zero we obtain the dispersion equation for the eigenmode spectrum. The determinant is factorized into three multipliers. The first multiplier yields the equation

$$\varepsilon_+(\mathbf{q}, \omega) = 1 - V_+(q)\Pi_{00}(\mathbf{q}, \omega) = 0. \quad (48)$$

Eq. (48) is the dispersion equation for the symmetric plasma excitation in the double layer system.

The dielectric function  $\varepsilon_+(\mathbf{q}, \omega)$  describes the screening of the scalar potential of a test charge  $\rho_+^{\text{test}}(\mathbf{q}, \omega)$ :

$$e^2 \varphi_+^{\text{src}}(\mathbf{q}, \omega) = \frac{V_+(q)}{\varepsilon_+(\mathbf{q}, \omega)} \rho_+^{\text{test}}(\mathbf{q}, \omega). \quad (49)$$

Eq. (49) follows from Eq. (43) written in the form  $e^2 \varphi_+^{\text{src}}(\mathbf{q}, \omega) = V_+(q)[\rho_+^{\text{test}}(\mathbf{q}, \omega) + \rho_+^{\text{ind}}(\mathbf{q}, \omega)]$ , where  $\rho_+^{\text{ind}}(\mathbf{q}, \omega) = e^2 \Pi_{00}(\mathbf{q}, \omega) \varphi_+^{\text{src}}(\mathbf{q}, \omega)$  is the induced charge.

From the continuity equation for the charge we obtain the relation between the polarization function  $\Pi_{00}(\mathbf{q}, \omega)$  and the longitudinal parallel current conductivity  $\sigma_{+,xx}(\mathbf{q}, \omega)$ :

$$\sigma_{+,xx}(q\mathbf{i}_x, \omega) = \frac{ie^2\omega}{q^2} \Pi_{00}(q\mathbf{i}_x, \omega), \quad (50)$$

where  $\mathbf{i}_x$  is the unit vector along the  $x$ -axis.

Considering the Maxwell equations with the corresponding boundary conditions and the matter equation for the current one can get the following dispersion equation for the symmetric plasmon modes<sup>32,37</sup>

$$1 + \frac{4\pi i \kappa_1}{\omega} \sigma_{+,xx}(q\mathbf{i}_x, \omega) + \frac{\varepsilon \kappa_1}{\kappa_2} \tanh \frac{\kappa_2 d}{2} = 0, \quad (51)$$

where  $\kappa_1 = \sqrt{q^2 - \omega^2/c^2}$  and  $\kappa_2 = \sqrt{q^2 - \varepsilon \omega^2/c^2}$ . Eq. (51) accounts retarded effects and due to this differs from Eq. (48). In the limit  $\kappa_1 = \kappa_2 = q$  that corresponds to nonretarded (plasmon) approximation Eq. (51) is reduced to Eq. (48).

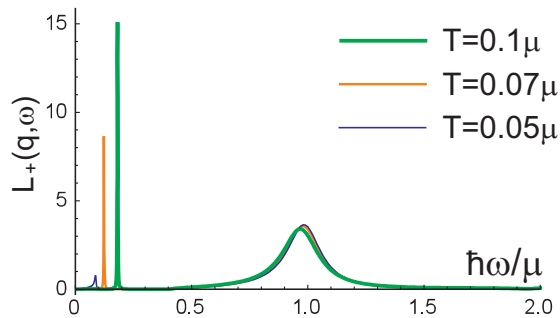


FIG. 1. Frequency dependence of the dielectric loss function (52) at  $T = 0.1\mu, 0.07\mu, 0.05\mu, q = 0.1k_F, \Delta = 0.2\mu$  and  $\gamma = 10^{-3}\mu$

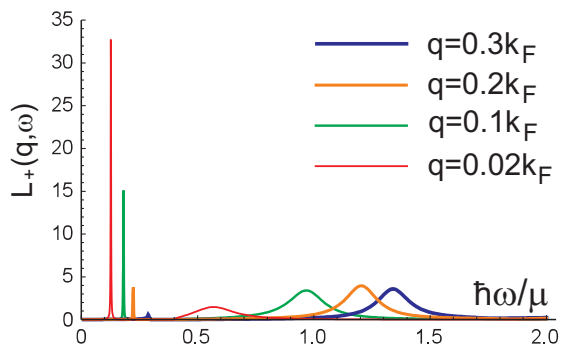


FIG. 2. Frequency dependence of the dielectric loss function (52) at  $T = 0.1\mu, q = 0.02k_F, 0.1k_F, 0.2k_F, 0.3k_F, \Delta = 0.2\mu$  and  $\gamma = 10^{-3}\mu$

Thus, we have shown that the order parameter oscillations are decoupled from the oscillations of  $\varphi_+$  and do not influence the spectrum of symmetric plasmon modes. The same result was obtained in Ref. 32 basing on the observation that the generalized Ward identity for the vertex function  $\Gamma_{\mu,+}$  is satisfied with bare vertexes (the vertexes  $\Gamma_{\mu,+}$  describe interaction of electrons with  $\varphi_+$  and  $\mathbf{A}_+$ , the sum of vector potentials of two layers). Therefore the Feynman diagram with the bare vertexes (which do not account order parameter oscillations) gives a gauge invariant polarization function  $\Pi_{00}$ .

In the general case Eq. (48) has two solutions<sup>32</sup>, one is below the gap ( $\hbar\omega < 2\Delta$ ), and the other, above the gap ( $\hbar\omega > 2\Delta$ ). It can be seen from the frequency dependence of the dielectric loss function. This function is defined as

$$L_+(\mathbf{q}, \omega) = -\text{Im} \left[ \frac{1}{\varepsilon_+(\mathbf{q}, \omega)} \right]. \quad (52)$$

It determines relative losses of energy of oscillations of a test charge  $\rho_+^{test}$ . The positions of peaks in the  $\omega$ -dependence of  $L_+(q, \omega)$  at fixed  $q$  correspond to the eigenmode frequencies. A half-width of the peak at its half-height gives the damping rate for the corresponding mode.

To compare the properties of symmetric and antisymmetric (see below) modes it is instructive to illustrate changes in the frequency dependence of  $L_+(\mathbf{q}, \omega)$  under variation of temperature (Fig. 1) and the wave vector (Fig. 2). One can see that the peak that corresponds to the lower mode disappears at small  $T$  and for large  $q$ . One can also see in Figs. 1 and 2 a wide peak that corresponds to the upper (strongly damped) mode. Note that at  $\Delta \rightarrow 0$  the damping rate of the upper mode decreases and this mode is transformed into the normal state optical plasmon mode.

The second multiplier in the determinant of the matrix in Eq. (45) yields the equation

$$\Pi_{11}^{(R)}(\mathbf{q}, \omega)\Pi_{22}^{(R)}(\mathbf{q}, \omega) + [\Pi_{12}(\mathbf{q}, \omega)]^2 = 0. \quad (53)$$

It is the dispersion equation for the excitations where only the difference  $\Delta_\uparrow - \Delta_\downarrow$  oscillates. Such oscillations are decoupled from the scalar potential oscillations.

In the theory of superconductivity the eigenmodes that correspond to oscillations of the phase and the modulus of the order parameter are known as the Anderson-Bogoliubov (AB) mode<sup>38,39</sup> and the Schmid<sup>40</sup> mode. Since in common superconductors the oscillations of the phase of the order parameter are coupled to plasma (scalar potential) oscillations, a genuine Anderson-Bogoliubov mode can emerge in neutral Fermi superfluids. In double layer systems with electron-hole pairing the presence of two superconducting components allows to realize the AB mode. To visualize the AB and the Schmid modes we introduce the functions

$$L_{11}(\mathbf{q}, \omega) = \frac{1}{g} \text{Im} \left[ \frac{1}{\Pi_{11}^{(R)}(\mathbf{q}, \omega) + \frac{[\Pi_{12}(\mathbf{q}, \omega)]^2}{\Pi_{22}^{(R)}(\mathbf{q}, \omega)}} \right], \quad (54)$$

$$L_{22}(\mathbf{q}, \omega) = \frac{1}{g} \text{Im} \left[ \frac{1}{\Pi_{22}^{(R)}(\mathbf{q}, \omega) + \frac{[\Pi_{12}(\mathbf{q}, \omega)]^2}{\Pi_{11}^{(R)}(\mathbf{q}, \omega)}} \right]. \quad (55)$$

These functions can be interpreted as analogs of the energy loss function (52). The functions  $L_{11}$  and  $L_{22}$  describe losses of energy under externally driven oscillations of the amplitude and the phase of the order parameter, correspondingly.

The frequency dependencies of  $L_{11}(\mathbf{q}, \omega)$  and  $L_{22}(\mathbf{q}, \omega)$  at three different  $q$  and  $T = 0.1\mu$  are shown in Fig. 3. One can see that the function  $L_{22}(\mathbf{q}, \omega)$ , Fig. 3b, has a peak at  $\hbar\omega < 2\Delta$ . The function  $L_{11}(\mathbf{q}, \omega)$ , Fig. 3a, has two peaks, one is at  $\hbar\omega < 2\Delta$  (at the same frequency as the peak in Fig. 3b) and the other, at  $\hbar\omega > 2\Delta$ . Two peaks in Fig. 3a appear due to the coupling of oscillations of the amplitude and the phase of the order parameter (in conventional superconductors these oscillations are decoupled from each other<sup>36</sup>). In Fig. 4 we present the same as in Fig. 3 dependencies at  $T = 0$ . One can see that the positions of the peaks remain practically unchanged under lowering of temperature (at  $\Delta = \text{const}$ ). At the same time an essential narrowing of the low-frequency peak at  $T = 0$  signals for a decrease of the damping rate of the lower mode. It is connected with that the Landau damping in the frequency domain  $\hbar\omega < 2\Delta$  is proportional to  $\exp(-\Delta/T)$ . On the contrary, in the frequency domain  $\hbar\omega > 2\Delta$  the Landau damping remains strong even at  $T = 0$ . Therefore the high-frequency peak is not changed under lowering of temperature.

The spectra of the modes determined by Eq. (53) are shown in Fig. 5. The dependencies presented are obtained from the position of the maximum of the functions (54) and (55) at  $T = 0$ . At small wave vectors the dispersion relation for the lower mode is approximated by the expression  $\omega = qv_F/\sqrt{2}$  that is the spectrum of the AB mode in two-dimensions. At large  $q$  the frequency of this mode approaches  $\omega = 2\Delta/\hbar$ . The frequency of the upper mode approaches  $2\Delta/\hbar$  at  $q \rightarrow 0$ . This mode can be recognized only in the limit  $q/k_F \ll 1$ . At  $q/k_F \gtrsim 0.2$  the peak that corresponds to the that mode washes out. The lower mode in Fig. 5 should be interpreted as an analog of the AB mode and the upper mode, as the analog of the Schmid mode.

The third multiplier in the determinant of the matrix in Eq. (45) yields the equation

$$\begin{aligned} & \left[ \Pi_{11}^{(R)}(\mathbf{q}, \omega)\Pi_{22}^{(R)}(\mathbf{q}, \omega) + [\Pi_{12}(\mathbf{q}, \omega)]^2 \right] [1 - V_-(q)\Pi_{33}(\mathbf{q}, \omega)] \\ & - V_-(q) \left[ \Pi_{11}^{(R)}(\mathbf{q}, \omega)[\Pi_{23}(\mathbf{q}, \omega)]^2 - \Pi_{22}^{(R)}(\mathbf{q}, \omega)[\Pi_{13}(\mathbf{q}, \omega)]^2 + 2\Pi_{12}(\mathbf{q}, \omega)\Pi_{13}(\mathbf{q}, \omega)\Pi_{23}(\mathbf{q}, \omega) \right] = 0. \end{aligned} \quad (56)$$

One can see that at  $V_-(q) = 0$  (that corresponds to  $d = 0$ ) Eq. (56) coincides with Eq. (53).

At  $V_-(q) \neq 0$  Eq. (56) can be rewritten in the form

$$\varepsilon_-(\mathbf{q}, \omega) = 1 - V_-(q)\Pi_-(\mathbf{q}, \omega) = 0, \quad (57)$$

where

$$\Pi_-(\mathbf{q}, \omega) = \Pi_{33}(\mathbf{q}, \omega) + \frac{\Pi_{11}^{(R)}(\mathbf{q}, \omega)[\Pi_{23}(\mathbf{q}, \omega)]^2 - \Pi_{22}^{(R)}(\mathbf{q}, \omega)[\Pi_{13}(\mathbf{q}, \omega)]^2 + 2\Pi_{12}(\mathbf{q}, \omega)\Pi_{13}(\mathbf{q}, \omega)\Pi_{23}(\mathbf{q}, \omega)}{\Pi_{11}^{(R)}(\mathbf{q}, \omega)\Pi_{22}^{(R)}(\mathbf{q}, \omega) + [\Pi_{12}(\mathbf{q}, \omega)]^2}. \quad (58)$$

The function  $\Pi_-(\mathbf{q}, \omega)$  can be understood as the polarization function "dressed" by the order parameter oscillations.

Eq. (57) is the dispersion equation for antisymmetric plasma oscillations coupled to the order parameter oscillations. The dielectric function  $\varepsilon_-(\mathbf{q}, \omega)$  determines screening of the scalar potential of a test charge  $\rho_-^{\text{test}}$ :  $e^2\varphi_-^{\text{src}}(\mathbf{q}, \omega) = V_-(q)\rho_-^{\text{test}}(\mathbf{q}, \omega)/\varepsilon_-(\mathbf{q}, \omega)$ .

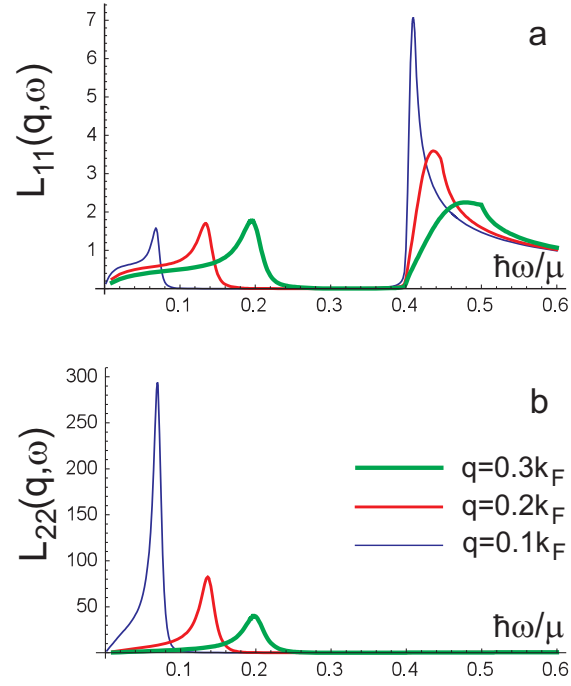


FIG. 3. Frequency dependence of the energy loss functions (54), (55) in  $\mu/gk_F^2$  units at  $T = 0.1\mu$ ,  $q = 0.1k_F, 0.2k_F, 0.3k_F$ ,  $\Delta = 0.2\mu$  and  $\gamma = 10^{-3}\mu$

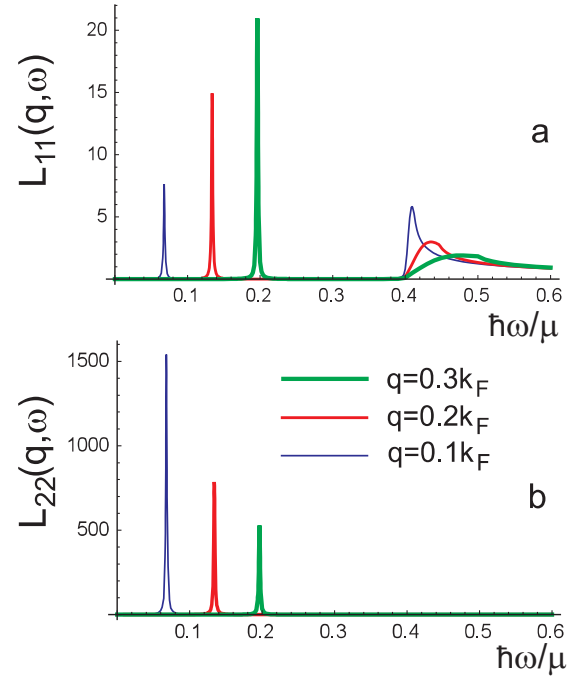


FIG. 4. The same as in Fig. 3 at  $T = 0$ .

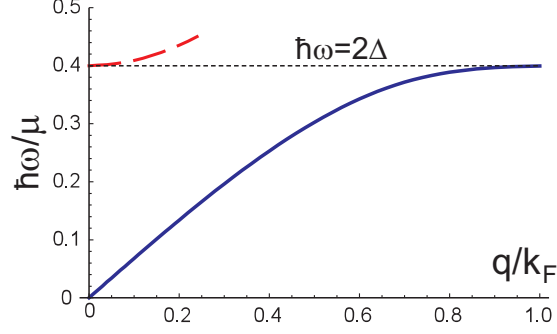


FIG. 5. The spectrum of the Anderson-Bogoliubov (solid curve) and Schmid (dashed curve) mode in the double layer graphene system.

The relation between the polarization function  $\Pi_-(\mathbf{q}, \omega)$  and the counterflow conductivity is given by the equation

$$\sigma_{-,xx}(q\mathbf{i}_x, \omega) = \frac{ie^2\omega}{q^2}\Pi_-(q\mathbf{i}_x, \omega). \quad (59)$$

The dispersion equation for the antisymmetric (acoustic) plasmon mode that accounts retarded effects has the form<sup>32,37</sup>

$$\left(1 + \frac{4\pi i\kappa_1\sigma_{-,xx}(q\mathbf{i}_x, \omega)}{\omega}\right) \tanh \frac{\kappa_2 d}{2} + \frac{\varepsilon\kappa_1}{\kappa_2} = 0. \quad (60)$$

In the nonretarded approximation ( $\kappa_1 = \kappa_2 = q$ ) Eq. (60) reduces to Eq. (57).

We analyze Eq. (57) considering the energy loss function

$$L_-(\mathbf{q}, \omega) = -\text{Im} \left[ \frac{1}{\varepsilon_-(\mathbf{q}, \omega)} \right]. \quad (61)$$

The frequency dependencies of  $L_-(\mathbf{q}, \omega)$  at four different wave vectors ( $q = 0.2k_F, 0.4k_F, 0.6k_F, 0.8k_F$ ),  $\Delta = 0.2\mu$ ,  $T = 0.1\mu$  and  $T = 0$  are shown in Fig. 6. The parameters used for the calculations are  $\varepsilon = 4$ ,  $dk_F = 0.1$  and  $\gamma = 10^{-3}\mu$ . One can see that in similarity with  $L_+(\mathbf{q}, \omega)$  the function  $L_-(\mathbf{q}, \omega)$  contains two peaks, one is below the gap  $2\Delta$  and the other, above the gap. The low-frequency peak is narrower than the high-frequency one. In difference with the  $L_+(\mathbf{q}, \omega)$ -dependence the position of the lower peak of the  $L_-(\mathbf{q}, \omega)$ -dependence remains practically unchanged under variation of temperature (at  $\Delta = \text{const}$ ). This peak does not disappear at  $T = 0$ .

In conventional superconductors the mode that corresponds to coupled oscillations of the scalar potential and the phase of the order parameter is known as the Carlson-Goldman (CG) mode<sup>41</sup>. The frequency of the CG mode satisfies the inequality  $\hbar\omega < 2\Delta$ . The mentioned similarities allows to interpret the lower antisymmetric mode an analog of the Carlson-Goldman mode.

Lowering of temperature results in a considerable decrease of the damping rate of the lower mode but does not influence the damping rate of the upper mode. As in the case of the AB and Schmid modes it is connected with the specific temperature and frequency dependence of the Landau damping in the state with electron-hole pairing<sup>32</sup>.

The dispersion curves calculated from the positions of two maximums of the function (61) at  $T = 0$  are shown in Fig. 7. The lower mode has the acoustic dispersion relation at small wave vectors. At large  $q$  its frequency approaches  $2\Delta/\hbar$ . The dispersion curve for the acoustic plasmon mode in the normal state ( $\Delta = 0$ ) calculated at the same parameters is also shown in Fig. 7. It is known<sup>42</sup> that the velocity  $v_a$  of the acoustic plasmon in a double-layer graphene system can be very close to  $v_F$ , but it is always larger than  $v_F$  irrespectively to the value of  $d$  and  $\varepsilon$ . For  $\varepsilon$  and  $d$  specified above  $v_a \approx 1.016v_F$ . The velocity of the CG mode  $v_{CG}$  can be smaller than  $v_F$ . In our case  $v_{CG} \approx 0.77v_F$ . The velocity  $v_{CG}$  is larger than the velocity of the AB mode  $v_{AB} = v_F/\sqrt{2}$  but there is no requirement for  $v_{CG}$  to be larger than  $v_F$ . It is correlates with the fact that in the normal state the mode with the phase velocity  $v_{ph} < v_F$  should experience strong Landau damping, but in the paired state the modes with  $\omega < 2\Delta$  do not experience Landau damping at  $T = 0$ .

At  $q/k_F > 0.9$  the peak at the  $L_-(\mathbf{q}, \omega)$ -dependence that corresponds to the CG mode disappears. On the contrary, the upper mode peak is well recognized at large  $q$ , while at small  $q$  this peak is almost disappears. At  $\Delta \rightarrow 0$  the

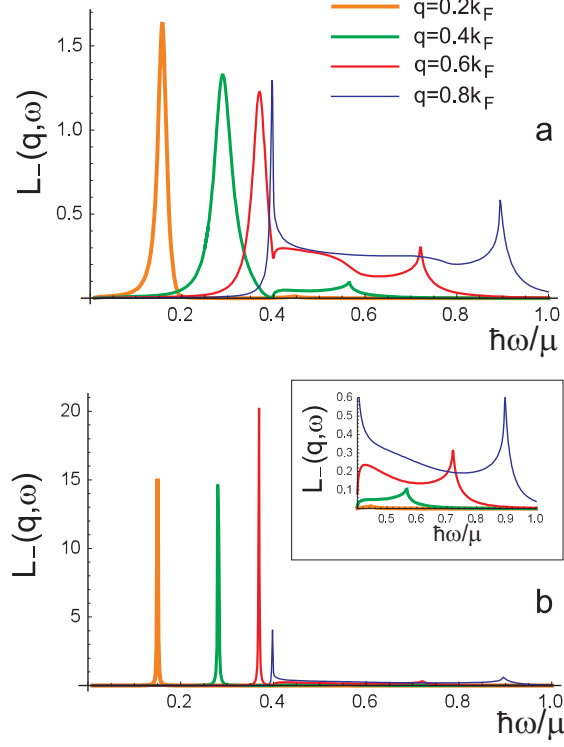


FIG. 6. Frequency dependence of the energy loss function (61) at  $T = 0.1\mu$  (a) and  $T = 0$  (b). The high-frequency peaks at  $T = 0$  are shown in the inset in another scale.

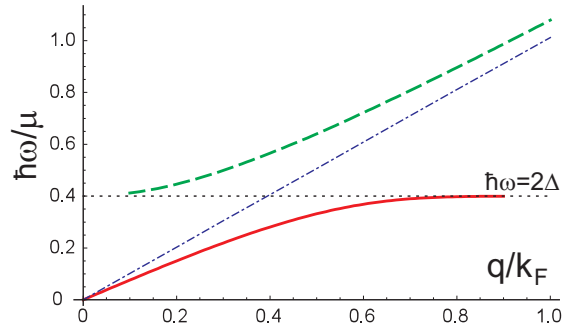


FIG. 7. The dispersion curves for the Carlson-Goldman mode (solid curve) and for the upper antisymmetric plasmon mode (dashed curve). The spectrum of the antisymmetric (acoustic) plasmon mode in the normal state is shown by the dash-dot line.

upper mode is transformed into the acoustic plasmon mode. It allows to interpret the upper antisymmetric mode as a residual acoustic plasmon mode.

## VI. CONCLUSION

In conclusion, we have shown that explicit accounting of the order parameter oscillations is crucial in obtaining the spectra of antisymmetric plasma modes in double layer systems with electron-hole pairing. At the same time the approach<sup>32</sup> based on a particular solution of the generalized Ward identity cannot describe a number of important

features. In particular, taking in account the order parameter oscillations we predict the existence of two antisymmetric modes. The upper mode can be interpreted as a residual normal state acoustic plasmon, and the lower mode, as an analog of the Carlson-Goldman mode. Two more modes interpreted as analogs of the Anderson-Bogoliubov and Schmid modes are also identified. The latter modes are associated with out of phase oscillations of the order parameters of two spin subsystems.

While the results are obtained with reference to a double monolayer graphene, one can expect that they reflect the general collective mode behavior in double layer systems with electron-hole pairing. Our approach can be easily extended to the double bilayer graphene systems<sup>20,21</sup>. The polarization functions for the double bilayer graphene are obtained from Eq. (37) under substitution  $\xi_{\mathbf{k},\lambda} \approx \lambda \hbar^2 k'^2 / 2m - \mu$  and  $\chi_{\mathbf{k}} \approx \mp 2\theta_{\mathbf{k}'}$ , where  $m$  is the effective mass. Preliminary calculations show that the collective mode systematics for the double bilayer graphene systems is the same as for the double monolayer ones. At the same time we emphasize that our approach is not applied to the systems with low density of carriers and a large gap between the valence and conducting bands. The counterflow superconductivity in the low density limit is described by the interacting boson model<sup>24,43,44</sup>. Such systems also have two superfluid components but the frequency of the mode that corresponds to out of phase oscillations of two components becomes imaginary-valued under increase of the interlayer distance<sup>24,44</sup>. It signals for an instability with respect to spatial separation of the components. The system considered in the present paper does not show softening of the out of phase mode and it is stable with respect to spatial separation.

### ACKNOWLEDGMENT

This study was supported by the grant of the Ukraine State Fund for Fundamental Research (project No. 33683).

- 
- \* fil@isc.kharkov.ua
- <sup>1</sup> S. I. Shevchenko, Fiz. Nizk. Temp. **2**, 505 (1976) [Sov. J. Low Temp. Phys. **2**, 251 (1976)].
  - <sup>2</sup> Yu. E. Lozovik and V. I. Yudson, Zh. Eksp. Teor. Fiz. **71**, 738 (1976) [Sov. Phys. JETP **44**, 389 (1976)].
  - <sup>3</sup> D. V. Fil and S. I. Shevchenko, Fiz. Nizk. Temp. **44**, 1111 (2018) [Low Temp. Phys. **44**, 867 (2018)].
  - <sup>4</sup> M. Kellogg, J. P. Eisenstein, L. N. Pfeiffer, and K. W. West, Phys. Rev. Lett. **93**, 036801 (2004).
  - <sup>5</sup> E. Tutuc, M. Shayegan, and D. A. Huse, Phys. Rev. Lett. **93**, 036802 (2004).
  - <sup>6</sup> R. D. Wiersma, J. G. S. Lok, S. Kraus, W. Dietsche, K. von Klitzing, D. Schuh, M. Bidder, H. - P. Tranitz, and W. Wegscheider, Phys. Rev. Lett. **93**, 266805 (2004).
  - <sup>7</sup> J. P. Eisenstein, Ann. Rev. Condensed Matter Phys. **5**, 159 (2014).
  - <sup>8</sup> I. B. Spielman, J. P. Eisenstein, L. N. Pfeiffer, and K. W. West, Phys. Rev. Lett. **87**, 036803 (2001).
  - <sup>9</sup> D. Nandi, A. D. K. Finck, J. P. Eisenstein, L. N. Pfeiffer, and K. W. West, Nature **488**, 481 (2012).
  - <sup>10</sup> A. F. Croxall, K. Das Gupta, C. A. Nicoll, M. Thangaraj, H. E. Beere, I. Farrer, D. A. Ritchie, and M. Pepper, Phys. Rev. Lett. **101**, 246801 (2008).
  - <sup>11</sup> J.A. Seamons, C. P. Morath, J. L. Reno, and M. P. Lilly, Phys. Rev. Lett. **102**, 026804 (2009).
  - <sup>12</sup> A. Gamucci, D. Spirito, M. Carrega, B. Karmakar, A. Lombardo, M. Bruna, L. N. Pfeiffer, K. W. West, A. C. Ferrari, M. Polini, and V. Pellegrini, Nat. Commun. **5**, 5824 (2014).
  - <sup>13</sup> G. W. Burg, N. Prasad, K. Kim, T. Taniguchi, K. Watanabe, A. H. MacDonald, L. F. Register, and E. Tutuc, Phys. Rev. Lett. **120**, 177702 (2018).
  - <sup>14</sup> Yu. E. Lozovik and A. A. Sokolik, Pis'ma v ZhETF **87** 61 (2008) [JETP Lett. **87**, 55 (2008)].
  - <sup>15</sup> H. Min, R. Bistritzer, J.-J. Su, and A. H. MacDonald, Phys. Rev. B **78**, 121401 (R) (2008)
  - <sup>16</sup> B. Seradjeh, H. Weber, and M. Franz, Phys. Rev. Lett. **101**, 246404 (2008).
  - <sup>17</sup> M. P. Mink, H. T. C. Stoof, R. A. Duine, and A. H. MacDonald, Phys. Rev. B **84**, 155409 (2011).
  - <sup>18</sup> I. Sodemann, D. A. Pesin, and A. H. MacDonald, Phys. Rev. B **85**, 195136 (2012).
  - <sup>19</sup> Yu. E. Lozovik, S. L. Ogarkov, and A. A. Sokolik, Phys. Rev. B **86**, 045429 (2012).
  - <sup>20</sup> A. Perali, D. Neilson, and A. R. Hamilton, Phys. Rev. Lett. **110**, 146803 (2013).
  - <sup>21</sup> J.-J. Su, A. H. MacDonald, Phys. Rev. B **95** 045416 (2017).
  - <sup>22</sup> S. Conti, A. Perali, F. M. Peeters, and D. Neilson, Phys. Rev. Lett. **119**, 257002 (2017).
  - <sup>23</sup> M. Zarenia, A. Perali, D. Neilson, and F.M. Peeters, Sci. Rep. **4** 7319 (2014).
  - <sup>24</sup> F. C. Wu, F. Xue, and A. H. MacDonald, Phys. Rev. B **92**, 165121 (2015).
  - <sup>25</sup> B. Debnath, Y. Barlas, D. Wickramaratne, M. R. Neupane, and R. K. Lake, Phys. Rev. B **96**, 174504 (2017).
  - <sup>26</sup> O. L. Berman and R. Ya. Kezerashvili, Phys. Rev. B, **96**, 094502 (2017).
  - <sup>27</sup> O. L. Berman, G. Gumbs, and R. Ya. Kezerashvili, Phys. Rev. B **96**, 014505 (2017).
  - <sup>28</sup> S. Saberi-Pouya, M. Zarenia, A. Perali, T. Vazifshenas, and F. M. Peeters Phys. Rev. B **97**, 174503 (2018).
  - <sup>29</sup> B. Seradjeh, J. E. Moore, and M. Franz, Phys. Rev. Lett. **103**, 066402 (2009).
  - <sup>30</sup> D. K. Efimkin, Yu. E. Lozovik, and A. A. Sokolik, Phys. Rev. B **86**, 115436 (2012).

- <sup>31</sup> K. V. Germash and D. V. Fil, Phys. Rev. B **91**, 115442 (2015).
- <sup>32</sup> K. V. Germash and D. V. Fil, Phys. Rev. B **93**, 205436 (2016).
- <sup>33</sup> K. V. Germash and D. V. Fil, EPL **118**, 67008 (2017).
- <sup>34</sup> Y. Nambu, Phys. Rev. **117**, 648 (1960).
- <sup>35</sup> J. R. Schrieffer, Theory of Superconductivity (Benjamin, New York, 1964).
- <sup>36</sup> I. O. Kulik, O. Entin-Wohlman, R. Orbach, J. Low Temp. Phys. **43**, 591 (1981).
- <sup>37</sup> Yu. V. Bludov, A. Ferreira, N. M. R. Peres, M. I. Vasilevskiy, Int. J. Mod. Phys. B **27**, 1341001 (2013).
- <sup>38</sup> P. W. Anderson, Phys. Rev. **112**, 1900 (1958).
- <sup>39</sup> N. N. Bogoljubov, V. V. Tolmachov, D. V. Shirkov, Fortschritte der Physik **6**, 605 (1958).
- <sup>40</sup> A. Schmid, Phys. kondens. Materie **8**, 129 (1968).
- <sup>41</sup> R. V. Carlson and A. M. Goldman, Phys. Rev. Lett. **34**, 11 (1975).
- <sup>42</sup> R. E. V. Profumo, R. Asgari, M. Polini, A. H. MacDonald, Phys. Rev. B **85**, 085443 (2012).
- <sup>43</sup> Yu. L. Lozovik and O. L. Berman, Zh. Eksp. Teor. Fiz. **111**, 1879 (1997) [J. Exp. Theor. Phys. **84**, 1027 (1997)].
- <sup>44</sup> D. V. Fil and S. I. Shevchenko, Fiz. Nizk. Temp. **42**, 1013 (2016) [Low Temp. Phys. **42**, 794 (2016)].